

Structure of vacancy-ordered single-crystalline superconducting potassium iron selenide

P. Zavalij,¹ Wei Bao,^{2,*} X. F. Wang,³ J. J. Ying,³ X. H. Chen,³ D. M. Wang,² J. B. He,² X. Q. Wang,² G. F. Chen,² P.-Y. Hsieh,⁴ Q. Huang,⁵ and M. A. Green^{4,5,†}

¹*Department of Chemistry, University of Maryland, College Park, Maryland 20742, USA*

²*Department of Physics, Renmin University of China, Beijing 100872, China*

³*Hefei National Laboratory for Physical Science at Microscale and Department of Physics, University of Science and Technology of China, Hefei, Anhui 230026, China*

⁴*Department of Materials Science and Engineering, University of Maryland, College Park, Maryland 20742, USA*

⁵*National Institute of Standards and Technology, Center for Neutron Research, 100 Bureau Dr., Gaithersburg, Maryland 20878, USA*

(Received 25 January 2011; revised manuscript received 10 February 2011; published 25 April 2011)

With single-crystal x-ray diffraction studies, we compare the structures of three samples showing optimal superconductivity: $\text{K}_{0.775(4)}\text{Fe}_{1.613(1)}\text{Se}_2$, $\text{K}_{0.737(6)}\text{Fe}_{1.631(3)}\text{Se}_2$, and $\text{Cs}_{0.748(2)}\text{Fe}_{1.626(1)}\text{Se}_2$. All have an almost identical ordered vacancy structure with a $(\sqrt{5} \times \sqrt{5} \times 1)$ supercell. The tetragonal unit cell, space group $I4/m$, possesses lattice parameters at 250 K of $a = b = 8.729(2)$ Å and $c = 14.120(3)$ Å, $a = b = 8.7186(12)$ Å and $c = 14.0853(19)$ Å, and at 295 K, $a = b = 8.8617(16)$ Å and $c = 15.304(3)$ Å for the three crystals, respectively. The structure contains two iron sites; one is almost completely empty while the other is fully occupied. There are similarly two alkali metal sites that are occupied in the range of 72.2(2)%–85.3(3)%. The inclusion of alkali metals and the presence of vacancies within the structure allows for considerable relaxation of the FeSe_4 tetrahedron, compared with members of the $\text{Fe}(\text{Te}, \text{Se}, \text{S})$ series, and the resulting shift of the Se-Fe-Se bond angles to less distorted geometry could be important in understanding the associated increase in the superconducting transition temperature. The structure of these superconductors are distinguished from the structure of the nonsuperconducting phases by an almost complete absence of Fe on the $(0\ 0.5\ 0.25)$ site, as well as lower alkali metal occupancy that ensures an exact Fe^{2+} oxidation state, which are clearly critical parameters in the promotion of superconductivity.

DOI: [10.1103/PhysRevB.83.132509](https://doi.org/10.1103/PhysRevB.83.132509)

PACS number(s): 74.70.Xa

A new series of superconductors with the general formula $\text{A}_x\text{Fe}_y\text{Se}_2$ has recently been identified and shown to have significantly enhanced superconducting transition temperatures (T_c up to 32 K)¹ as compared to FeSe ($T_c \approx 8.5$ K).² This series joins a growing list of pnictide and chalcogenide superconductors that includes the original ZrCuSiAs -type compounds, such as $\text{LnO}_{1-x}\text{F}_x\text{FeAs}$,^{3–9} where Ln is a lanthanide ion, the ThCr_2Si_2 -type structures of AFe_2As_2 , where A is an alkali or alkaline earth metal^{10–12} and the anti-PbFCl structure of AFeAs , where A is an alkali metal.^{13,14} All of these compounds contain iron in tetrahedral coordination that are edge-shared to form two-dimensional structures. The simplest of the chalcogenides are those with the anti-PbO structure with the general formula $\text{Fe}_{1+x}(\text{Te}, \text{Se}, \text{S})$. FeSe is superconducting at 8.5 K (Ref. 2) and is very sensitive to interstitial iron ions.¹⁵ Fe_{1+x}Te , where x lies between 0.076 and 0.18, shows commensurate or incommensurate antiferromagnetism, depending on the exact composition.¹⁶ The antiferromagnetism can be suppressed, and superconductivity emerges on substituting some Te with either Se (Refs. 17 and 18) or S (Ref. 19). In both cases, the chemical pressure afforded by the Se (Ref. 20) and S (Ref. 21) inclusion reduces the amount of interstitial iron. The amount of the interstitial iron can be reduced by topotactic deintercalation using iodine.²² $\text{Fe}_{1+x}\text{Te}_{0.7}\text{Se}_{0.3}$ was shown to transform from gapless paramagnetism to superconductivity on Fe removal.²³

The superconducting K-Fe-Se phases were found to possess the ThCr_2Si_2 structure and are isostructural with AFe_2As_2 .¹ The first structural determination of AFeSe in this layered tetragonal arrangement was with A as the group 13 metal, Tl. It possesses lattice parameters of $a = b = 3.890(1)$ Å

and $c = 14.00(1)$ Å and was shown to be a p-type Pauli paramagnetic metal.^{24–26} A related composition was shown to be antiferromagnetic at $T_N \approx 450$ K and have ordered Fe vacancies, which is best described as $\text{TlFe}_{2-x}\text{Se}_2$ with a $\sqrt{5} \times \sqrt{5} \times 1$ supercell giving a fivefold volume increase at $x \approx 0.3$.²⁷ Superconducting potassium iron selenide was first reported above 30 K in $\text{K}_x\text{Fe}_2\text{Se}_2$, which has K deficiency but stoichiometric Fe and Se, and lattice parameters of $a = 3.9136(1)$ Å and $c = 14.0367(7)$ Å.¹ Similar properties have also been reported in iron-deficient $(\text{Tl}, \text{K})\text{Fe}_x\text{Se}_2$,²⁸ alkali metal-deficient $\text{Rb}_{0.8}\text{Fe}_2\text{Se}_2$,²⁹ $\text{K}_x\text{Fe}_2\text{Se}_2$,³⁰ and $\text{K}_{0.8}\text{Fe}_{2.3}\text{Se}_2$,³¹ and alkali metal- and Se-deficient $\text{Rb}_{0.78}\text{Fe}_2\text{Se}_{1.78}$ (Ref. 32) and $\text{Cs}_{0.8}(\text{FeSe}_{0.98})_2$ (Ref. 33).

As a result of both the critical importance of interstitial iron in the $\text{Fe}_{1+x}(\text{Te}, \text{Se}, \text{S})$ series and the variation of properties in the $\text{A}_x\text{Fe}_y\text{Se}_2$ series, careful determination of the exact stoichiometry of these superconductors is warranted. In a single-crystal x-ray diffraction structure determination, we observe that in superconducting samples of composition $\text{K}_{0.775(4)}\text{Fe}_{1.613(1)}\text{Se}_2$, $\text{K}_{0.737(6)}\text{Fe}_{1.631(3)}\text{Se}_2$, and $\text{Cs}_{0.748(2)}\text{Fe}_{1.626(1)}\text{Se}_2$, with a near perfect diamagnetic response,^{31,34} an ordered vacancy structure that contains both alkali metal and iron deficiencies to form an ordered $(\sqrt{5} \times \sqrt{5} \times 1)$ superlattice exists, which is consistent with a recent transmission electron microscope study that reports a superstructure modulation along the $[310]$ direction,³⁵ as well as powder neutron diffraction.³⁶ The structure is related to a recent x-ray diffraction study of nonsuperconducting $\text{K}_{0.8+x}\text{Fe}_{1.6-y}\text{Se}_2$, but here we show that the superconducting composition contained one occupied and one vacant site rather

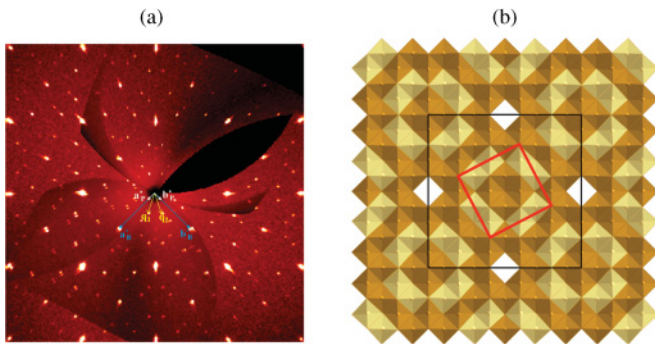


FIG. 1. (Color online) Panel (a) Single Crystal X-ray Diffraction pattern of $\text{K}_{0.775(4)}\text{Fe}_{1.613(1)}\text{Se}_2$ showing the relationship between the original ThCr_2Si_2 cell of approximate dimensions 3.9 \AA and 14 \AA indicated by vectors a_B^* and b_B^* can be interpreted in $(5 \times 5 \times 1)$ cell labeled, a_{rmp}^* and b_P^* . Alternatively q_1 and q_2 represent two alternative twinned cell with $(\sqrt{5} \times \sqrt{5} \times 1)$ as proposed by Haggstrom *et al.*²⁷ Panel (b) Diagrammatic representation of the structure in real space showing the $(5 \times 5 \times 1)$ cell (black) compared with the reduced $(\sqrt{5} \times \sqrt{5} \times 1)$ cell (red).

than two partially occupied Fe sites.³⁷ The complexity of the structure demonstrates the need to map out the iron selenide phase diagram with great precision to evaluate the structure-property relations.

The single crystals used in this study were synthesized by first reacting Fe and Se to form FeSe, which was subsequently reacted with K or Cs in a similar manner to that previously reported. Previous papers have reported superconductivity for the crystals, $\text{K}_{0.775(4)}\text{Fe}_{1.613(1)}\text{Se}_2$,³⁴ $\text{K}_{0.737(6)}\text{Fe}_{1.631(3)}\text{Se}_2$,³¹ and $\text{Cs}_{0.748(2)}\text{Fe}_{1.626(1)}\text{Se}_2$.³⁸ The x-ray intensity data at 250 K of metallic black platelike crystals of $\text{K}_{0.775(4)}\text{Fe}_{1.613(1)}\text{Se}_2$ and $\text{K}_{0.737(6)}\text{Fe}_{1.631(3)}\text{Se}_2$ and at 295 K for $\text{Cs}_{0.748(2)}\text{Fe}_{1.626(1)}\text{Se}_2$ were measured on a Bruker Smart Apex2, CCD system equipped with a graphite monochromator and a Mo $K\alpha$ fine-focus sealed tube ($\lambda = 0.71073 \text{ \AA}$). The exact details of the refinements are given in crystal structure reports in supplementary information.

The initial diffraction pattern for the very similar potassium and cesium iron selenide crystals, shown in Fig. 1, could be indexed on a 25 times two-dimensional modulation of the ThCr_2Si_2 structure. Initially crystal structure determination was performed in the supercell within space group $I4/mmm$. The latter was selected based on the intensity statistics. The resulting structure shown in Fig. 1, panel b contains six Fe sites; four are fully occupied, one is fully vacant, while one is partially occupied for about 40%. The final R -factor was 3.3% for the K-containing structure. However, these results were inconsistent with the initial model proposed by Haggstrom *et al.* for the related $\text{TlFe}_{2-x}\text{Se}_x$ structure,²⁷ recent NMR work that suggested limited iron site disorder from partial occupancy,³⁸ and powder neutron diffraction data.³⁶ In particular, the powder diffraction data, which can very accurately determine Fe composition in these systems,^{22,23} was refined in the $I4/m$ space group, using the original $(\sqrt{5} \times \sqrt{5} \times 1)$ superlattice. In addition, irreducible representation analysis of the magnetic structure in the 25 times cell suggested a reduced ab moment in two of the Fe sites that was unphysical and warranted more detailed investigation. Further analysis of

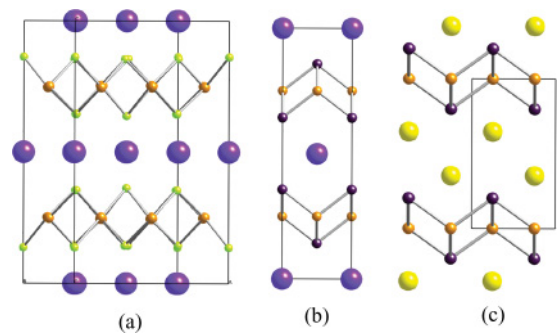


FIG. 2. (Color online) Comparison of the (a) $A_x\text{Fe}_{1-x/2}\text{Se}_2$ structure with the same body centered ThCr_2Si_2 -type stacking as (b) BaFe_2As_2 rather than the primitive anti-PbFCl structure of (c) NaFeAs .

the crystal structure in the light of other measurements showed that the structure can be represented in the $(\sqrt{5} \times \sqrt{5} \times 1)$ cell with the lower $I4/m$ space group, with the presence of twinning (180° rotation around 100 axis) with approximately 1:1 ratio of twin components. This structure then yields an ordered distribution of the two Fe sites, such that one is almost completely empty and one is fully occupied. The relationship between the two cells is shown in Fig. 1, panel b.

On the final stages of refinement of both K and Cs structures, the difference Fourier maps showed the presence of electron density in the almost empty Fe sites on the level of 1-2 electrons. When placing Fe atoms in this site with all occupation factors including factors of K or Cs refined independently, the resulting composition satisfied the charge balance very accurately (within one standard deviation). Thus the general formula could be written as $A_x\text{Fe}_{1-x/2}\text{Se}_2$ ($A = \text{K}, \text{Cs}$), and in the final refinement the occupation of Fe and M were constrained to match this composition exactly. The final R -factor was 1.9%, 3.38%, and 3.02% for $\text{K}_{0.775(4)}\text{Fe}_{1.613(1)}\text{Se}_2$, $\text{K}_{0.737(6)}\text{Fe}_{1.631(3)}\text{Se}_2$, and $\text{Cs}_{0.748(2)}\text{Fe}_{1.626(1)}\text{Se}_2$ crystals, respectively.

A diagrammatic representation of the structure of these alkali metal iron selenides that possesses similar body-centered

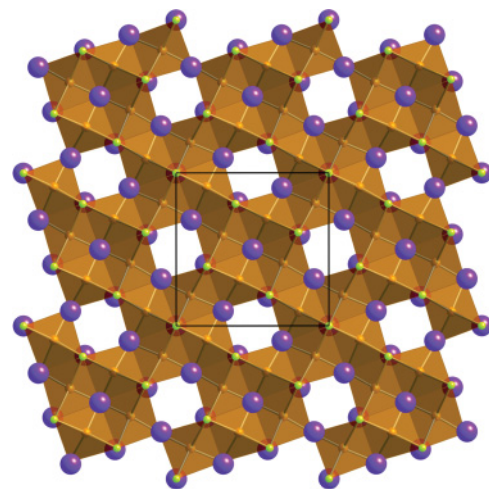


FIG. 3. (Color online) Structure of $\text{K}_{0.775(4)}\text{Fe}_{1.613(1)}\text{Se}_2$ from the $[001]$ direction in the $(\sqrt{5} \times \sqrt{5} \times 1)$ cell showing fully occupied Fe sites (orange) decorated with ordered vacancy sites.

TABLE I. Summary of atomic coordinates and some selected bond angles in the tetragonal $I4/m$ cell for the superconducting phases, $K_{0.775(4)}Fe_{1.613(1)}Se_2$, $K_{0.737(6)}Fe_{1.631(3)}Se_2$, and $Cs_{0.748(2)}Fe_{1.626(1)}Se_2$. A represents either K or Cs. Atomic positions are at A_1 (0 0 0.5), A_2 (x , y , 0.5), Fe_1 (0 0.5 0.25), Fe_2 (x , y , z), Se_1 (0 0 z), and Se_2 (x , y , z). Both A positions are partially occupied. Fe_1 is occupied with very low amounts, whereas Fe_2 has full occupancy in all refinements.

	$K_{0.737(6)}Fe_{1.631(3)}Se_2$	$K_{0.775(4)}Fe_{1.613(1)}Se_2$	$Cs_{0.748(2)}Fe_{1.626(1)}Se_2$
A_1 U	0.0343(11)	0.0337(6)	0.0402(4)
A_1 occ	0.790(4)	0.838(4)	0.853(3)
A_2 x	0.8082(3)	0.808 17(17)	0.807 87(11)
A_2 y	0.4021(3)	0.402 07(15)	0.405 53(9)
A_2 U	0.0317(7)	0.0292(4)	0.0370(2)
A_2 occ	0.724(7)	0.759(4)	0.722(2)
Fe_1 U	0.017(6)	0.014(7)	0.007(4)
Fe_1 occ	0.078(7)	0.032(4)	0.065(2)
Fe_2 x	0.301 49(8)	0.301 60(4)	0.301 60(8)
Fe_2 y	0.408 56(11)	0.409 00(6)	0.408 55(9)
Fe_2 z	0.246 96(7)	0.246 74(3)	0.247 91(5)
Fe_2 U	0.0178(2)	0.014 49(11)	0.020 17(17)
Se_1 z	0.137 87(10)	0.137 43(5)	0.147 91(8)
Se_1 U	0.0177(2)	0.014 47(12)	0.0199(2)
Se_2 x	0.110 74(12)	0.111 18(7)	0.110 22(8)
Se_2 y	0.299 68(6)	0.299 72(3)	0.297 98(6)
Se_2 z	0.354 80(4)	0.354 69(2)	0.344 34(3)
Se_2 U	0.019 22(15)	0.016 23(8)	0.021 76(13)
a (Å)	8.729(2)	8.7186(12)	8.8617(16)
c (Å)	14.120(3)	14.0853(19)	15.304(3)
T (K)	250(2)	250(2)	295(2)
Se–Fe–Se	107.79(5)° 113.62(4)°	108.06(3)° 113.62(2)° 113.76(2)°	109.28(4)° 112.98(4)°
bond angles	113.69(3)° 106.89(6)°	106.60(3)° 113.774(18)°	112.60(3)° 105.66(4)°
	113.71(4)° 100.97(6)°	100.79(3)°	112.69(3)° 103.37(4)°

$ThCr_2Si_2$ stacking to $BaFe_2As_2$ are compared with the primitive symmetry of anti-PbFCl structure of $NaFeAs$ in Fig. 2. These structures have the same morphology as $BaFe_2As_2$. However, the five times larger cell now has two crystallographic inequivalent positions for potassium, iron, and selenium. Of these two iron positions, one Fe site at (0 0.5 0.25) is almost completely empty for all three superconducting structures, while the other on a general position is fully occupied. A list of the atomic coordinates is given in Table I.

The Se–Fe–Se bond angles have extensive distribution ranging from 100.79° to 113.76°, but with a number of bond angles remarkably close to the ideal tetrahedron angle of 109.47°. This far less distorted arrangement than in the related Fe(Te, Se, S) series may offer an explanation to the considerably higher superconducting transition temperature; the sensitivity of the superconducting transition temperature with the iron anion tetrahedron has been suggested for the iron-based superconductors.^{39–41}

The two iron sites in both the K and Cs superconducting crystals have very different occupancies. The general Fe $16i$ site is fully occupied, while there is very low occupancy of the $4d$ site, which is in contrast to that observed for nonsuperconducting samples.³⁷ Although the refinement of the $4d$ Fe occupancy made a notable improvement to the fit, such low levels of iron (3.2%–7.8%) may not be a bulk effect or homogeneously distributed within the crystal. Such occupancies could, for example, arise from small domains,

such as near the crystal surface, which support the occupancy of the $4d$ site, leaving the rest of the crystal without $4d$ iron. In either the case of the presence of domains or where the crystal possesses a homogeneous distribution of $4d$ iron, this arrangement is grossly different to that observed for nonsuperconducting samples in Ref. 37. Two significant differences can be highlighted between the superconducting and nonsuperconducting compositions. First, the nonsuperconducting samples contain significantly more alkali metal and less iron, although both are nominal charge balanced and possess Fe^{2+} ions. More importantly, the superconducting samples have different iron distribution across the two sites, with almost all occupying the general $16i$ site in preference to the $4d$ site, which will create crucial differences in the resulting electronic structure. Fig. 3 shows a diagrammatic representation of the vacancy ordered structure in $K_{0.775(4)}Fe_{1.613(1)}Se_2$.

In summary, we determined the crystal structure of two superconducting analogs of an $A_xFe_{1-x/2}Se_2$ ($A = K, Cs$) system. They possess $I4/m$ symmetry with a $(\sqrt{5} \times \sqrt{5} \times 1)$ cell compared with the related $ThCr_2Si_2$ structure, which is created through ordered vacancies of the Fe within the Fe–Se planes, yielding examples of a high-temperature superconductor with structural holes within the superconducting layers. The iron atoms have a strong tendency to sit on the general $16i$ positions, leaving the other $4d$ sites almost completely empty, in contrast to similar composition that do not possess superconductivity. Control of the both the alkali metal and

iron compositions within the structure will be crucial in establishing a phase diagram that maps superconductivity and antiferromagnetism.

Work at RUC was supported by the National Basic Research Program of China (973 Program) under Grants No. 2011CBA00112, No. 2010CB923000, No. 2009CB009100,

and No. 2007CB925001, and by the National Science Foundation of China under Grants No. 11034012, No. 10834013, No. 10874244, and No. 10974254. Work at CUST was supported by the National Science Foundation of China, the Ministry of Science and Technology of China, and the Chinese Academy of Sciences.

*wbao@ruc.edu.cn.

†mark.green@nist.gov.

¹J. Guo, S. Jin, G. Wang, S. Wang, K. Zhu, T. Zhou, M. He, and X. Chen, *Phys. Rev. B* **82**, 180520 (2010).

²F. C. Hsu *et al.*, *Proc. Natl. Acad. Sci. USA* **105**, 14262 (2008).

³Y. Kamihara, T. Watanabe, M. Hirano, and H. Hosono, *J. Am. Chem. Soc.* **130**, 3296 (2008).

⁴G. F. Chen, Z. Li, D. Wu, G. Li, W. Z. Hu, J. Dong, P. Zheng, J. L. Luo, and N. L. Wang, *Phys. Rev. Lett.* **100**, 247002 (2008).

⁵Z. A. Ren *et al.*, *EPL* **82**, 57002 (2008).

⁶Z. A. Ren *et al.*, *Chin. Phys. Lett.* **25**, 2215 (2008).

⁷Z. A. Ren, J. Yang, W. Lu, W. Yi, G. C. Che, X. L. Dong, L. L. Sun, and Z. X. Zhao, *Mater. Res. Innovations* **12**, 105 (2008).

⁸X. H. Chen, T. Wu, G. Wu, R. H. Liu, H. Chen, and D. F. Fang, *Nature* **453**, 761 (2008).

⁹R. H. Liu *et al.*, *Phys. Rev. Lett.* **101**, 087001 (2008).

¹⁰M. Rotter, M. Tegel, and D. Johrendt, *Phys. Rev. Lett.* **101**, 107006 (2008).

¹¹G. F. Chen *et al.*, *Chin. Phys. Lett.* **25**, 3403 (2008).

¹²Y. Qiu *et al.*, *Phys. Rev. Lett.* **101**, 257002 (2008).

¹³M. J. Pitcher, D. R. Parker, P. Adamson, S. J. C. Herkelrath, A. T. Boothroyd, R. M. Ibberson, M. Brunelli, and S. J. Clarke, *Chem. Commun.* 5918 (2008).

¹⁴X. C. Wang, Q. Q. Liu, Y. X. Lv, W. B. Gao, L. X. Yang, R. C. Yu, F. Y. Li, and C. Q. Jin, *Solid State Commun.* **148**, 538 (2008).

¹⁵T. M. McQueen *et al.*, *Phys. Rev. B* **79**, 014522 (2009).

¹⁶W. Bao *et al.*, *Phys. Rev. Lett.* **102**, 247001 (2009).

¹⁷K. W. Yeh *et al.*, *EPL* **84**, 37002 (2008).

¹⁸M. H. Fang, H. M. Pham, B. Qian, T. J. Liu, E. K. Vehstedt, Y. Liu, L. Spinu, and Z. Q. Mao, *Phys. Rev. B* **78**, 224503 (2008).

¹⁹Y. Mizuguchi, F. Tomioka, S. Tsuda, T. Yamaguchi, and Y. Takano, *Appl. Phys. Lett.* **94**, 012503 (2009).

²⁰B. C. Sales, A. S. Sefat, M. A. McGuire, R. Y. Jin, D. Mandrus, and Y. Mozharivskij, *Phys. Rev. B* **79**, 094521 (2009).

²¹P. Zajdel, P.-Y. Hsieh, E. E. Rodriguez, N. P. Butch, J. D. Magil, J. Paglione, P. Zavalij, M. R. Suchomel, and M. A. Green, *J. Am. Chem. Soc.* **132**, 13000 (2010).

²²E. E. Rodriguez, P. Zavalij, P. Y. Hsieh, and M. A. Green, *J. Am. Chem. Soc.* **132**, 10006 (2010).

²³E. E. Rodriguez, C. Stock, P.-Y. Hsieh, N. Butch, J. Paglione, and M. A. Green, e-print [arXiv:1012.0590](https://arxiv.org/abs/1012.0590) (to be published).

²⁴K. O. Klepp and H. Boller, *Monatsch. Chem.* **109**, 1049 (1978).

²⁵G. Brun, B. Gardes, J. Tedenac, A. Raymond, and M. Maurin, *Mater. Res. Bull.* **14**, 743 (1979).

²⁶R. Berger and C. Van Bruggen, *J. Less-Common Met.* **99**, 113 (1984).

²⁷L. Haggstrom, H. Verma, S. Bjarman, R. Wappling, and R. Berger, *J. Solid State Chem.* **63**, 401 (1986).

²⁸M. Fang, H. Wang, C. Dong, C. Feng, J. Chen, and H. Q. Yuan, e-print [arXiv:1012.5236](https://arxiv.org/abs/1012.5236) (to be published).

²⁹B. Shen, F. Han, X. Zhu, and H.-H. Wen, e-print [arXiv:1012.5637](https://arxiv.org/abs/1012.5637) (to be published).

³⁰Y. Mizuguchi, H. Takeya, Y. Kawasaki, T. Ozaki, S. Tsuda, T. Yamaguchi, and Y. Takano, e-print [arXiv:1012.4950](https://arxiv.org/abs/1012.4950) (to be published).

³¹D. M. Wang, J. B. He, T.-L. Xia, and G. F. Chen, e-print [arXiv:1101.0789](https://arxiv.org/abs/1101.0789) (to be published).

³²A. F. Wang *et al.*, e-print [arXiv:1012.5525](https://arxiv.org/abs/1012.5525) (to be published).

³³A. Krzton-Maziopa, Z. Shermadini, E. Pomjakushina, V. Pomjakushin, M. Bendele, A. Amato, R. Khasanov, H. Luetkens, and K. Conder, e-print [arXiv:1012.3637](https://arxiv.org/abs/1012.3637) (to be published).

³⁴J. J. Ying *et al.*, e-print [arXiv:1012.5552](https://arxiv.org/abs/1012.5552) (to be published).

³⁵Z. Wang *et al.*, e-print [arXiv:1101.2059](https://arxiv.org/abs/1101.2059) (to be published).

³⁶W. Bao, Q. Huang, G. F. Chen, M. A. Green, D. M. Wang, J. B. He, X. Q. Wang, and Y. Qiu, e-print [arXiv:1102.0830](https://arxiv.org/abs/1102.0830) (to be published).

³⁷J. Bacsá, A. Y. Ganin, Y. Takabayashi, K. E. Christensen, K. Prasad, M. J. Rosseinsky, and J. B. Claridge, e-print [arXiv:1102.0488](https://arxiv.org/abs/1102.0488) (to be published).

³⁸W. Yu, L. Ma, J. B. He, D. M. Wang, T.-L. Xia, and G. F. Chen, e-print [arXiv:1101.1017](https://arxiv.org/abs/1101.1017) (to be published).

³⁹J. Zhao *et al.*, *Nature Mater.* **7**, 953 (2008).

⁴⁰A. Kreyssig *et al.*, *Phys. Rev. B* **78**, 184517 (2008).

⁴¹C. H. Lee *et al.*, *J. Phys. Soc. Jpn.* **77**, 083704 (2008).